Lyapunov-based Optimizing Control of Nonlinear Blending Process

Tor A. Johansen*, Daniel Sbárbaro**

*Department of Engineering Cybernetics, Norwegian University of Science and Technology, 7491 Trondheim, Norway.

**Department of Electrical Engineering, University of Concepción, Concepción, Chile.

Abstract

Blending processes consisting of linear dynamics and a static nonlinearity are considered. We propose a control law that optimizes the equilibrium point of the process and regulates the output to the corresponding equilibrium state. The analysis and design also incorporates the use of an observer for state and bias estimation. Experimental results using a laboratory scale colorant blending process illustrate the efficiency of the method.

I. Introduction

Blending processes arise in a wide range of industries, for example gasoline blending [1], [2], [3], [4], food, pharmaceuticals and colorant blending [5], [6], [7]. They are characterized by fairly simple dynamics, essentially transport delays due to piping in addition to linear blending dynamics. However, such processes contain static nonlinearities that describe the relationship between the composition of the mixture (i.e. the concentrations of its individual substances) and the output variables (the overall quality measure of the mixture). Hence, a blending controller needs to take into account these nonlinearities in order to achieve a mixture with the given quality specification. A further complication is that the composition of the mixture can usually not be measured directly, so there is a need for a state estimator or observer. Optimization of the use of raw materials is also desirable, especially if the number of feed components are larger than the number of output variables, which is the more common situation.

In this work we develop and analyze an optimization-based control technique for such nonlinear blending processes, which we assume are described by a linear time-invariant state-space model plus a static output nonlinearity. The idea is based on a control Lyapunov function (CLF) that is augmented by a steady-state optimization criterion that ensures that the quality measure of the mixture is according to specification, the cost of raw materials is minimized, and a barrier function that ensures that the steady-state operating point does not violate any feed pump constraints. Based on this CLF and a dynamic control specification, an optimizing

This work was supported by Fondecyt, Chile, Project 700397.

Corresponding author: Tor.Arne.Johansen@itk.ntnu.no

controller is derived similar to CLF design of adaptive and nonlinear controllers [8]. After this basic control strategy is developed, we extend the controller with an observer that takes into account that the state is not measured, and there are unknown output disturbances. Stability, convergence and asymptotic optimality of the closed loop is then proved under general conditions. The use of the suggested method is illustrated using a laboratory scale colorant blending process where three colorants are blended to give a required color, for example specified in terms of its RGB values. A preliminary version of the method suggested here was presented in [9], and the idea of seeking only asymptotic optimality is similar to [10] and the sub-optimal approach [11]. The approach provides an alternative control method for systems of the Wiener class, as treated recently in [12], [13], [14].

II. Colorant blending process

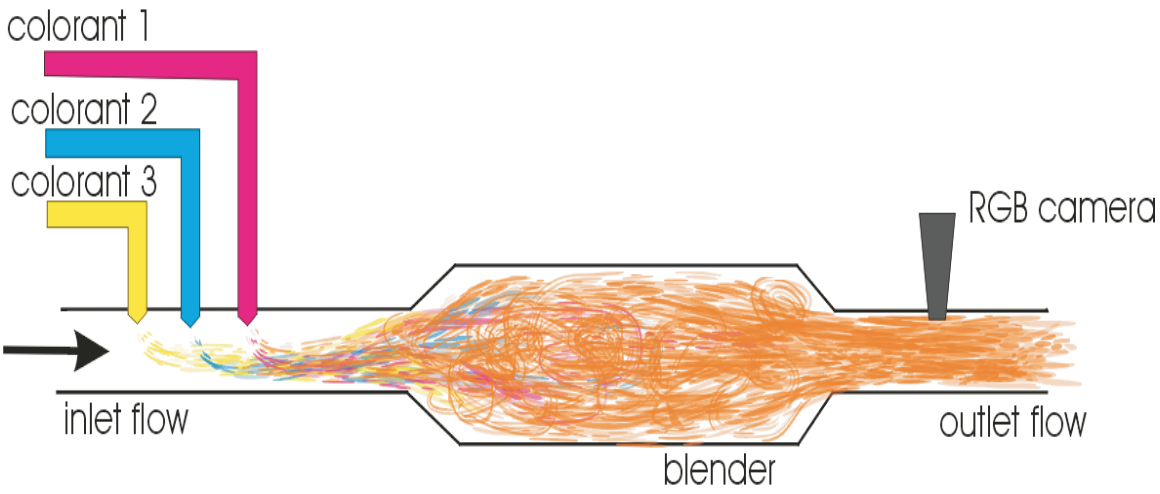

Fig. 1. Colorant blending process.

Consider the laboratory scale colorant blending process illustrated in Figure 1. The inlet flow contains water from the water supply. The flow rate may be controlled, but is subject to disturbances caused by variations in the supply pressure due to load transients. The inlet flow is mixed with three different colorants, whose flow rate can be controlled via the speeds of individual pumps. The blender unit contains baffles that leads to a non-stationary flow pattern that gives good spatial mixing. At the outlet of the blender there is an RGB camera and an illumination source, confined in a closed environment, that provides a measurement of the color of the mixture. The RGB image is processed to determine an average RGB value for the mixture.

Let $u \in \mathbb{R}^3$ denote the colorant pump speeds, $z \in \mathbb{R}^3$ denote the concentration of the three colorants at the camera position, and $y \in \mathbb{R}^3$ denote the measured RGB values (y_1 is red, y_2 is green, and y_3 is blue). Experiments show that the dynamic response from each colorant pump speed to the corresponding concentration at the blender outlet can be accurately described by a first order linear system with dead-time

$$\frac{z_i}{u_i}(s) \quad = \quad \frac{e^{-3.5s}}{1+3s} \tag{1}$$

In this transfer function, the units of z_i are non-physical units for colorant concentrations, and $z = u$ as steady-state. The steady-state mapping $y = g(u)$ from pump speeds to RGB values can be described theoretically by the Kubelka-Munk theory and a sensor model [15]. However, since the parameters of these models are not easily identified, we propose a parameterized nonlinear mapping described by polynomials of the form:

$$y_i = a_{i1}u_1 + a_{i2}u_2 + a_{i3}u_3 + a_{i4}u_1^2 + a_{i5}u_2^2 + a_{i6}u_3^2 + a_{i7}u_1u_2 + a_{i8}u_1u_3 + a_{i9}u_2u_3 + a_{i10} \quad (2)$$

for $i = 1, 2, 3$. The parameters used in the experiments are identified from measured data, and given in Table I.

i	1	2	3
a_{i1}	-0.168597	-0.617673	-0.703415
a_{i2}	-0.815173	-0.593565	-0.236830
a_{i3}	0.159001	0.192853	-0.097820
a_{i4}	0.000437	0.001010	0.001358
a_{i5}	0.001442	0.000853	0.000256
a_{i6}	-0.000106	-0.000342	0.000067
a_{i7}	0.000331	0.000723	0.000512
a_{i8}	-0.000652	-0.000609	0.000092
a_{i9}	-0.000074	0.000137	0.000181
a_{i10}	216.92	228.17	193.38

TABLE I

ESTIMATED PARAMETERS OF STATIC NONLINEARITY IN THE LABORATORY COLORANT BLENDING PROCESS.

In this paper an optimization-based nonlinear controller will be first developed and analyzed within a theoretical framework in sections III and IV. For the purpose of this analysis the nonlinear model of the blending process is written in the state-space form

$$\dot{x} = Ax + Bu \quad (3)$$

$$y = g(x) \quad (4)$$

where $x \in \mathbb{R}^n$, $u \in \mathbb{R}^m$ and $y \in \mathbb{R}^m$. For the colorant blending process above, $m = 3$. We remark that g is a continuously differentiable nonlinear function, and (A, B) is controllable and open-loop stable. For the purpose of the analysis, the time-delay can be assumed to be approximated with a finite-dimensional linear time-invariant system incorporated in (3). In the experimental implementation used with the laboratory process, a discrete-time formulation is used which can directly incorporate the time-delay, see section V.

III. State feedback optimizing controller

Let $\theta \in \mathbb{R}^m$ denote the equilibrium input, to be optimized, and ξ be the corresponding equilibrium state for (3) such that

$$0 \quad = \quad A\xi + B\theta \tag{5}$$

It follows that there exists a matrix F such that $\xi = F\theta$. The control strategy is to employ a linear state feedback where the reference and feed-forward are defined from the equilibrium input θ that is optimized such that the equilibrium output equals it reference value $g(F\theta) = y^*$. In other words, the objective is to choose θ such that it minimizes the steady-state performance criterion

$$J(\theta; y^*) \quad = \quad \frac{1}{2}\left(y^* - g(F\theta)\right)^T W \left(y^* - g(F\theta)\right) \tag{6}$$

where $W > 0$ is a symmetric weighting matrix. In general, this criterion should also include the cost of raw materials (usually a linear term in θ). However, with the laboratory colorant blending process there are no additional degrees of freedom (only 3 colorants) such that this is meaningless. We refer to [9] for a simulation example considering the more general situation. Finally, the dynamic performance specification is given in terms of an infinite-horizon LQ criterion with $Q > 0$, and $R > 0$:

$$J_{LQ}(u; x(t), \theta) \quad = \quad \int_t^\infty \left((x(\tau) - F\theta)^T Q (x(\tau) - F\theta) + (u(\tau) - \theta)^T R (u(\tau) - \theta)\right) d\tau \tag{7}$$

Hence, the controller objective is to simultaneously optimize the equilibrium point and achieve regulation to the optimal equilibrium.

Assume a compact and convex constraint set $\Theta_c \subset \mathbb{R}^m$ is given. Such a convex set can be derived from input constraints such as $u_{min} \leq u \leq u_{max}$ which means the equilibrium input θ must satisfy $u_{min} \leq \theta \leq u_{max}$. Let the interior of Θ_c be denoted int(Θ_c), its boundary be denoted $\partial\Theta_c$ and assume the set Θ_c is represented as

$$\Theta_c \quad = \quad \{\theta \in \mathbb{R}^m \mid c(\theta) \leq 0\} \tag{8}$$

The set of vectors $\theta \in \Theta_c$ satisfying first order optimality conditions is defined in terms of the Karush-Kuhn-Tucker (KKT) conditions [16]:

$$\Theta_c^* \quad = \quad \left\{ \theta \in \Theta_c \;\middle|\; \nabla_\theta J(\theta; y^*) + \sum_{i=1}^{q} \lambda_i \nabla c_i(\theta) = 0,\ \lambda_i c_i(\theta) = 0,\ \lambda_i \geq 0 \right\} \tag{9}$$

Define the logarithmic barrier function

$$b(\theta) \quad = \quad b_0 - \sum_{i=1}^{q} \log(-c_i(\theta)) \tag{10}$$

where the constant $b_0 \in \mathbb{R}$ is selected such that $b(\theta) > 0$ for all $\theta \in$ int(Θ_c). Such a b_0 exists due to the compactness of Θ_c. A fundamental property of this barrier function is that it is well-defined and convex on int(Θ_c) since Θ_c is convex [17]. Moreover, its

value goes to infinity as $\theta \to \partial\Theta_c$, and it is undefined outside Θ_c. Next, define a CLF

$$V(x,\theta,\varrho) \quad = \quad (x-F\theta)^T P(x-F\theta) + \beta\left(J(\theta;y^*) + \varrho b(\theta)\right) + \frac{1}{2}\varrho^2 \tag{11}$$

where $P > 0$ and $\beta > 0$ will be specified shortly. For all weighting parameters $\varrho > 0$ the barrier function will prevent $\theta(t)$ from escaping the interior of Θ_c. When applying such barrier functions in numerical optimization, convergence toward the optimum is usually achieved by letting $\varrho \to 0$ as $t \to \infty$, [16], [17], and we take a similar approach here (at least for the theoretical analysis in this section):

$$\dot{\varrho} \quad = \quad -\nu\varrho \tag{12}$$

with $\nu > 0$. The time-derivative of V along trajectories of the closed loop system is given by

$$\dot{V} \quad = \quad (x-F\theta)^T\left((PA+A^TP)x + 2PBu - 2PF\dot{\theta}\right) + \beta\nabla_\theta^T J(\theta;y^*)\dot{\theta} + \beta\varrho\nabla^T b(\theta)\dot{\theta} + \dot{\varrho}b(\theta) + \dot{\varrho}\varrho \tag{13}$$

We choose the optimizing dynamic feedback

$$\dot{\theta} \quad = \quad -\Gamma\ell(\theta,\varrho;y^*) \tag{14}$$

with $\Gamma > 0$ and $\ell(\theta,\varrho;y^*) = \nabla_\theta J(\theta;y^*) + \varrho\nabla b(\theta)$. The control input is chosen according to the LQ controller

$$u \quad = \quad -R^{-1}B^TP(x-F\theta) + \theta \tag{15}$$

and the matrix $P \succ 0$ satisfies the algebraic Riccati equation

$$A^TP + PA - 2PBR^{-1}B^TP \quad = \quad -Q \tag{16}$$

This leads to

$$\dot{V} \quad = \quad -(x-F\theta)^TQ(x-F\theta) - \beta\ell^T(\theta,\varrho;y^*)\Gamma\ell(\theta,\varrho;y^*) - \nu\varrho b(\theta) - \nu\varrho^2 + 2(x-F\theta)^TPF\Gamma\ell(\theta,\varrho;y^*) \tag{17}$$

The indefinite term in (17) is dominated by the negative quadratic terms as shown in the proof of the following result:

Proposition 1: Consider the optimizing controller described above and assume Θ_c is a convex and compact set. Then this controller has the following properties for all $x(0) \in \mathbb{R}^n$, $\theta(0) \in \text{int}(\Theta_c)$ and $\varrho(0) > 0$:

1. If J is strictly convex, then $\Theta_c^* = \{\theta^*\}$, the equilibrium point $(x,\theta,\varrho) = (F\theta^*,\theta^*,0)$ is asymptotically stable, and $g(x(t)) \to y^*$ as $t \to \infty$.

2. If J is radially unbounded, then all variables are uniformly bounded and $\theta(t) \in \text{int}(\Theta_c)$ for all $t \geq 0$. Moreover, $\theta(t) \to \Theta_c^*$, and $||x(t) - F\theta(t)|| \to 0$ as $t \to \infty$.

Proof. Using Young's inequality $2ab \leq a^2/k + b^2k$ for $k > 0$, (17) implies

$$\dot{V} \quad \leq \quad -||x-F\theta||^2(\underline{\sigma}(Q) - 2k\overline{\sigma}(PF\Gamma)) - ||\ell(\theta,\varrho;y^*)||^2(\underline{\sigma}(\Gamma)\beta - 2\overline{\sigma}(PF\Gamma)/k) - \nu\varrho^2 - \nu\varrho b(\theta) \tag{18}$$

The first term is made negative by choosing the arbitrary constant $k > 0$ sufficiently small. The second term is made negative by choosing the arbitrary constant $\beta > 0$ sufficiently large. Notice that $\varrho(t) = \varrho(0)\exp(-\beta t)$ such that $\varrho(t) > 0$ for all $t \geq 0$. Since $b(\theta)$ goes unbounded and all other terms remain bounded when θ approaches the boundary of Θ_c, it is clear that $\theta(t) \in \text{int}(\Theta_c)$ for all $t \geq 0$. Hence, the last term in (18) is non-positive because $b(\theta)$ is positive for all $\theta \in \text{int}(\Theta_c)$. It follows immediately that $\dot{V}(t) \leq 0$ for all $t \geq 0$ and $||\varrho(t)b(\theta(t))||$, $||x(t) - F\theta(t)||$, $|\varrho(t)|$ and $||\ell(\theta(t), \varrho(t); y^*)||$ are uniformly bounded.

In part 1, θ^* is a unique global minimum due to strict convexity, and we have

$$\begin{aligned} E &= \{(x, \theta, \varrho) \in \mathbb{R}^n \times \Theta_c \times [0, \infty) \mid \dot{V}(x, \theta, \varrho) = 0\} \\ &= \{(x, \theta, \varrho) \in \mathbb{R}^n \times \Theta_c \times [0, \infty) \mid \varrho = 0,\ \varrho b(\theta) = 0,\ x = F\theta,\ \nabla_\theta J(\theta; y^*) + \varrho \nabla b(\theta) = 0\} \end{aligned} \tag{19}$$

Elementary calculations show

$$\nabla b(\theta) = -\sum_{i=1}^{q} \frac{\nabla c_i(\theta)}{c_i(\theta)} \tag{20}$$

Define the vector $\lambda \in \mathbb{R}^q$ in terms of its components (which can be interpreted as Lagrange multipliers, see also [16]):

$$\lambda_i = -\frac{\varrho}{c_i(\theta)} \tag{21}$$

which is well-defined since $\theta \in \text{int}(\Theta_c)$. Hence, the last condition in (19) can be written

$$\ell(\theta, \varrho; y^*) = \nabla_\theta J(\theta; y^*) + \lambda^T \nabla c(\theta) = 0 \tag{22}$$

Since $\varrho \geq 0$ and $c(\theta) < 0$ for all $\theta \in \text{int}(\Theta_c)$, it follows that $\lambda \geq 0$. Hence, the 1st and 3rd KKT condition in (9) are satisfied. Since $\varrho = 0$ the 2nd KKT condition is also satisfied due to (21), and we conclude that $\theta = \theta^*$ in (19). It follows that $E = \{(\theta^*, \xi^*, 0)\}$ and part 1 of the proposition is proven by Barbashin-LaSalle's theorem [18].

Part 2 can be proven as follows. Since b is locally Lipschitz in $\text{int}(\Theta_c)$ the conditions of Barbalat's lemma hold [18], and we conclude that $\dot{V}(t) \to 0$ as $t \to \infty$ such that (18) implies

$$\varrho(t) \to 0, \quad \text{as} \quad t \to \infty \tag{23}$$

$$\varrho(t)b(\theta(t)) \to 0, \quad \text{as} \quad t \to \infty \tag{24}$$

$$||x(t) - F\theta(t)|| \to 0, \quad \text{as} \quad t \to \infty \tag{25}$$

$$||\nabla_\theta J(\theta(t); y^*) + \varrho(t)\nabla b(\theta(t))|| \to 0, \quad \text{as} \quad t \to \infty \tag{26}$$

As above, with $\lambda_i(t) = -\varrho(t)/c_i(\theta(t))$, it is clear that (26) implies

$$\nabla_\theta J(\theta(t); y^*) + \sum_{i=1}^{q} \lambda_i(t) \nabla c_i(\theta(t)) \to 0, \quad \text{as} \quad t \to \infty \tag{27}$$

Because all functions are continuous in int(Θ_c) and (23) implies $\lambda_i(t)c_i(\theta(t)) \to 0$ as $t \to \infty$ for all $i \in \{1, 2, ..., q\}$, it is evident that all KKT conditions in (9) hold asymptotically. Since $\lambda_i(t) > 0$ for all $t \geq 0$, we conclude $\theta(t) \to \Theta_c^*$ as $t \to \infty$.

□

With constant gain matrix $\Gamma \succ 0$, (14) corresponds to a gradient descent minimization. Notice, however, that Γ in (14) can be replaced by any time- or state-dependent positive definite-matrix, such as a possibly modified inverse Hessian of J, leading to a Newton-method, in order to improve speed of convergence [16]. In a discrete-time implementation, a line search method is useful to adapt the gain such that descent and convergence are guaranteed.

IV. Observer-based optimizing controller

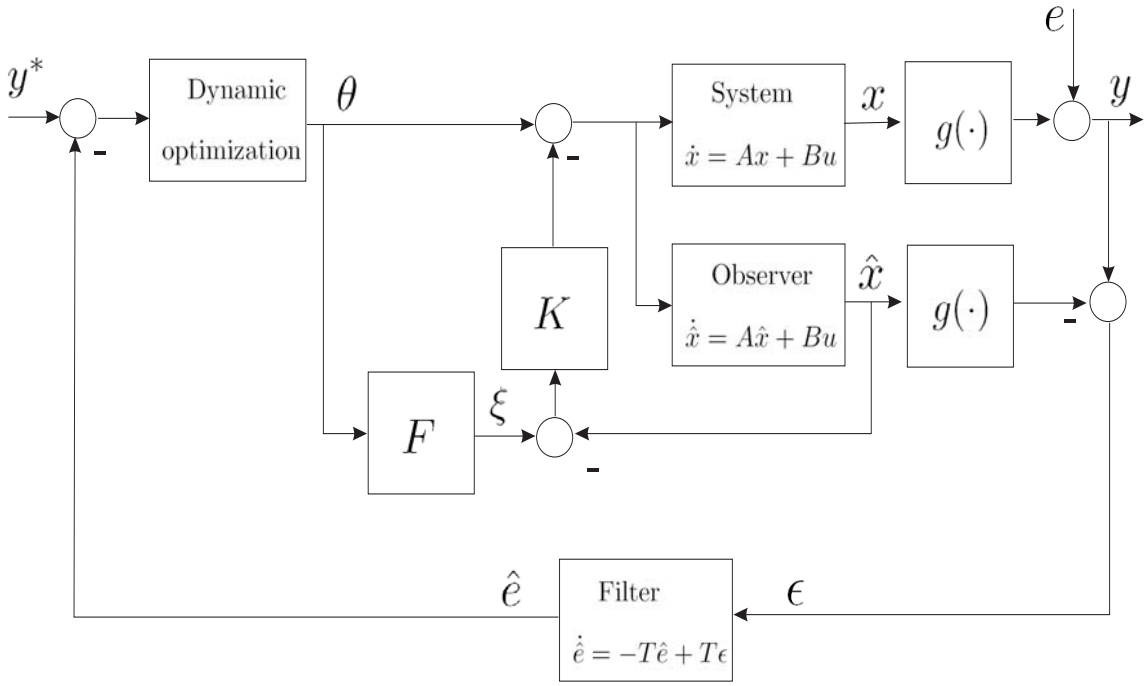

Fig. 2. Observer-based optimizing controller for the nonlinear blending process.

The CLF design of the controller and optimizer in section III does not take into account that the state cannot in general be measured. Furthermore, the colorant feed pumps, water supply pressure, colorant feed compositions and the output map g are subject to significant uncertainty. In order to avoid steady-state error due to this uncertainty it is necessary with feedback from the measured color y. This is achieved through an observer that estimates the state x and the output bias e, defined by the equation $y = g(x) + e$, and a controller that compensates for this bias. We therefore describe a closely related observer-based optimizing controller that utilizes the Internal Model Control (IMC) principle [19] and shows that the observer cannot destabilize the control system. Without loss of generality, we neglect the constraints in the analysis in this section for simplicity. Since the blending process is in general open loop stable, we employ an open-loop observer for x. Assuming the bias e is an unknown constant and y^*

is a constant output reference, the closed loop system illustrated in Figure 2 containing the plant, observer, controller and dynamic optimization is described by the following set of differential and algebraic equations

$$\dot{x} = Ax + Bu \tag{28}$$

$$y = g(x) + e \tag{29}$$

$$\dot{\hat{x}} = A\hat{x} + Bu \tag{30}$$

$$\dot{\hat{e}} = -T\hat{e} + T(y - g(\hat{x})) \tag{31}$$

$$\dot{\theta} = -\Gamma\nabla_\theta J(\theta, y^* - \hat{e}) \tag{32}$$

$$u = -K(F\theta - \hat{x}) + \theta \tag{33}$$

where $K = R^{-1}B^TP$. The observer gains are tuned via the diagonal matrix $T > 0$. The following result shows that the observer and control errors converge under mild conditions:

Proposition 2: Suppose A is Hurwitz, g is Lipschitz, and there exist a constant $\kappa_1 > 0$ such that $\nabla g(x)F \geq \kappa_1 I$. Then for any initial conditions all signals are bounded, and the trajectories of the closed loop system (28)-(33) converges such that $\hat{x}(t) \to x(t)$, $\hat{e}(t) \to e$, $\theta(t) \to \Theta^*$, $x(t) \to F\theta(t)$, and $y(t) \to y^*$ as $t \to \infty$.

Proof: Consider the following Lyapunov function candidate

$$V(x, \hat{x}, \theta, e) = (\hat{x} - F\theta)^TP(\hat{x} - F\theta) + \beta J(\theta, y^* - \hat{e}) + (x - \hat{x})^T\Lambda(x - \hat{x}) + (e - \hat{e})^TS(e - \hat{e}) \tag{34}$$

where $\beta < 0$ and symmetric matrices $P > 0$, $S > 0$ and $\Lambda > 0$ will be specified later. Differentiating with respect to time along trajectories of the closed loop system gives

$$\begin{aligned}
\dot{V} &= 2(\dot{\hat{x}} - F\dot{\theta})^TP(\hat{x} - F\theta) + \beta\nabla_\theta^T J(\theta, y^* - \hat{e})\dot{\theta} - \beta\nabla_{y^*}^T J(\theta, y^* - \hat{e})\dot{\hat{e}} + 2(\dot{x} - \dot{\hat{x}})^T\Lambda(x - \hat{x}) + 2(\dot{e} - \dot{\hat{e}})^TS(e - \hat{e}) \\
&= 2((A + BK)(\hat{x} - F\theta) - F\dot{\theta})^TP(\hat{x} - F\theta) - \beta\dot{\theta}^T\Gamma^{-1}\dot{\theta} + \beta\nabla_{y^*}^T J(\theta, y^* - \hat{e})(T\hat{e} - T(g(x) + e - g(\hat{x}))) \\
&\quad + (x - \hat{x})^T(A^T\Lambda + \Lambda A)(x - \hat{x}) - (e - \hat{e})^T(T^TS + ST)(e - \hat{e} + g(x) - g(\hat{x})) \\
&= -(\hat{x} - F\theta)Q(\hat{x} - F\theta) - 2\dot{\theta}^TF^TP(\hat{x} - F\theta) - \beta\dot{\theta}^T\Gamma^{-1}\dot{\theta} - \beta\nabla_{y^*}^T J(\theta, y^* - \hat{e})T(e - \hat{e}) \\
&\quad - \beta\nabla_{y^*}^T J(\theta, y^* - \hat{e})T(g(x) - g(\hat{x})) - (e - \hat{e})^T(T^TS + ST)(g(x) - g(\hat{x})) \\
&\quad + (x - \hat{x})^T(A^T\Lambda + \Lambda A)(x - \hat{x}) - (e - \hat{e})^T(T^TS + ST)(e - \hat{e})
\end{aligned} \tag{35}$$

where $P > 0$ satisfies the Lyapunov equation

$$(A + BK)^TP + P(A + BK) = -Q \tag{36}$$

for some arbitrary $Q > 0$. Recall that

$$\dot{\theta} = -\Gamma \nabla_\theta J(\theta, y^* - \hat{e}) = \Gamma \left(\nabla g(F\theta) F\right)^T W (y^* - \hat{e} - g(F\theta)) \quad (37)$$

$$= \Gamma \left(\nabla g(F\theta) F\right)^T \nabla_{y^*} J(\theta, y^* - \hat{e}) \quad (38)$$

Hence,

$$\nabla_{y^*} J(\theta, y^* - \hat{e}) = -(F^T \nabla^T g(F\theta))^{-1} \Gamma^{-1} \dot{\theta} \quad (39)$$

Using the multi-variable version of Taylor's theorem, [20], we have $g(x) - g(\hat{x}) = \nabla g(\tilde{x})(x - \hat{x})$ for some $\tilde{x}$ on the line segment between x and $\hat{x}$. We now define

$$\mathbb{Y}(x, \hat{x}, \theta) = -\frac{1}{2} T \left(F^T \nabla^T g(F\theta)\right)^{-1} \Gamma^{-1} \quad (40)$$

such that $\dot{V}$ can be written in the following form

$$\begin{aligned} \dot{V} &= -(\hat{x} - F\theta) Q (\hat{x} - F\theta) - \beta \dot{\theta}^T \Gamma^{-1} \dot{\theta} + (x - \hat{x})^T (A^T \Lambda + \Lambda A)(x - \hat{x}) - (e - \hat{e})^T (T^T S + S T)(e - \hat{e}) \\ &\quad -2\dot{\theta}^T F^T P (\hat{x} - F\theta) + 2\beta \dot{\theta}^T \mathbb{Y}^T \nabla g(\tilde{x})(x - \hat{x}) + 2\beta \dot{\theta}^T \mathbb{Y}^T (e - \hat{e}) + (e - \hat{e})^T (T^T S + S T) \nabla g(\tilde{x})(x - \hat{x}) \quad (41) \\ &\leq -||\hat{x} - F\theta||^2 \underline{\sigma}(Q) - ||\dot{\theta}||^2 \beta \underline{\sigma}(\Gamma^{-1}) - ||x - \hat{x}||^2 \underline{\sigma}(-A^T \Lambda - \Lambda A) - ||e - \hat{e}||^2 \underline{\sigma}(T^T S + S T) \\ &\quad +2||\dot{\theta}|| \cdot ||\hat{x} - F\theta|| \overline{\sigma}(F^T P) + 2||\dot{\theta}|| \cdot ||x - \hat{x}|| \beta L_g \overline{\sigma}(\mathbb{Y}) + 2||\dot{\theta}|| \cdot ||e - \hat{e}|| \beta \overline{\sigma}(\mathbb{Y}) \\ &\quad +2||e - \hat{e}|| \cdot ||x - \hat{x}|| \overline{\sigma}(ST) L_g \quad (42) \end{aligned}$$

where L_g is the Lipschitz constant for g. Using Young's inequality $2ab \leq a^2/k + b^2 k$, where $k > 0$ is arbitrary, gives

$$\begin{aligned} \dot{V} &\leq -||\hat{x} - F\theta||^2 \left(\underline{\sigma}(Q) - \overline{\sigma}(F^T P)\mu_1\right) \\ &\quad -||\dot{\theta}||^2 \left(\beta \underline{\sigma}(\Gamma^{-1}) - \overline{\sigma}(F^T P)/\mu_1 - \beta L_g \overline{\sigma}(\mathbb{Y})\mu_2 - \beta \overline{\sigma}(\mathbb{Y})\mu_2\right) \\ &\quad -||x - \hat{x}||^2 \left(\underline{\sigma}(-A^T \Lambda - \Lambda A) - \beta L_g \overline{\sigma}(\mathbb{Y})/\mu_2 - L_g \overline{\sigma}(ST)\right) \\ &\quad -||e - \hat{e}||^2 \left(\underline{\sigma}(T^T S + S T) - \beta \overline{\sigma}(\mathbb{Y})/\mu_2 - L_g \overline{\sigma}(ST)\right)\big) \quad (43) \end{aligned}$$

where $\mu_1, \mu_2 > 0$ are arbitrary. At this point, recall that in addition to μ_1 and μ_2, one can choose freely the following parameters that arise in the analysis only (their values have no implications or relevance for the control design or tuning): $\Lambda > 0$, $S > 0$, and $\beta > 0$. We proceed as follows:

1. Choose μ_1 sufficiently small such that $\underline{\sigma}(Q) - \overline{\sigma}(F^T P)\mu_1 > 0$.

2. Choose μ_2 sufficiently small and β sufficiently large such that $\beta \underline{\sigma}(\Gamma^{-1}) - \overline{\sigma}(F^T P)/\mu_1 - \beta L_g \overline{\sigma}(\mathbb{Y})\mu_2 - \beta \overline{\sigma}(\mathbb{Y})\mu_2 > 0$. This is in general possible because $\mathbb{Y}$ is bounded.

3. Choose Λ sufficiently large such that $\underline{\sigma}(-A^T \Lambda - \Lambda A) - \beta L_g \overline{\sigma}(\mathbb{Y})/\mu_2 - \overline{\sigma}(ST) L_g > 0$.

4. Choose S so large that $\underline{\sigma}(T^T S + ST) - \beta\overline{\sigma}(\mathbb{Y})/\mu_2 - \overline{\sigma}(ST)L_g > 0$.

It follows that $\dot{V}(t) \leq 0$ for all $t \geq 0$ such that all signals are bounded, and Barbalat's lemma immediately gives convergence. Notice that $\dot{\theta}(t) \to \infty$ implies $\nabla_\theta J(\theta(t), y^* - \hat{e}(t)) \to 0$ such that $\theta(t) \to \Theta^*$ as $t \to \infty$.

□

We remark that the assumptions are reasonable: A is indeed Hurwitz for the process under consideration, and blending processes in general. The assumption on positive definiteness of $\nabla g(x)F$ and g being Lipschitz is verified to hold for the output map for the colorant process given in section II for all states of interest. We also mention that the filter time constant $T > 0$ can be replaced by a time-varying $T(t) > 0$ without affecting the convergence results.

V. Experimental results

The implementation of the controller has three interesting differences compared to the theory outlined in sections III and IV. First, a discrete-time model is used in the observer, such that the dead-time can be implemented exactly. The sampling interval is $T_s = 0.5$ sec. Second, a dead-time compensation scheme similar to [21] is employed. This means that we apply feedback from the observed non-delayed state. This essentially corresponds to a partial state feedback through the gain matrix K. Proposition 2 still holds, since open loop stability of the plant implies existence of a $P > 0$ in the proof. Finally, we have chosen the barrier function weight $\varrho(t) = 0.25$, rather than letting it go to zero asymptotically. This is done in order to avoid numerical problems, and its only consequence is that the input constraints will hold with some insignificant small margin.

The tuning of the controller is done as follows. The feedback gain matrix K is chosen via an LQ design (based on a discrete-time state-space model without time-delay since the feedback is from the observed non-delayed states). Since the time-delay dominates the dynamics, the design parameters are chosen such that the gain is small in order to achieve a high degree of robustness. The IMC filter time constant T is replaced by a rate-limiter (the theory still holds for any time-varying $T(t) > 0$) in order not to introduce unnecessary phase loss. The optimizer gain $\Gamma(t) = \gamma(t)I$ is chosen as $\gamma(t) = 2.5$, but the value is reduced, if necessary, in a line search phase to achieve descent. The pumps' speed are limited at the minimum value 60 rpm, and the maximum value 260 rpm. The weighting matrix is $W = I$.

Experimental results are shown in Figures 3 - 5. The RGB reference makes several simultaneous step changes throughout the experiment, and we observe that there is accurate tracking and disturbance rejection. The asymptotic optimization converges quickly, and imposes no significant loss of performance. The bias estimates show that the model of the static nonlinearity is far from an ideal model, yet the bias estimation scheme works well and avoids steady-state tracking error. At time $t = 140$ sec a 25 % increase in water supply flow rate occurs, leading to a significant disturbance on the process. The bias estimator detects the resulting output bias (see Figure 5) and the disturbance only leads to a fairly small transient on the RGB output. At time $t = 185$ sec the water supply flow rate goes back to its original value, and another small transient results. The results with the

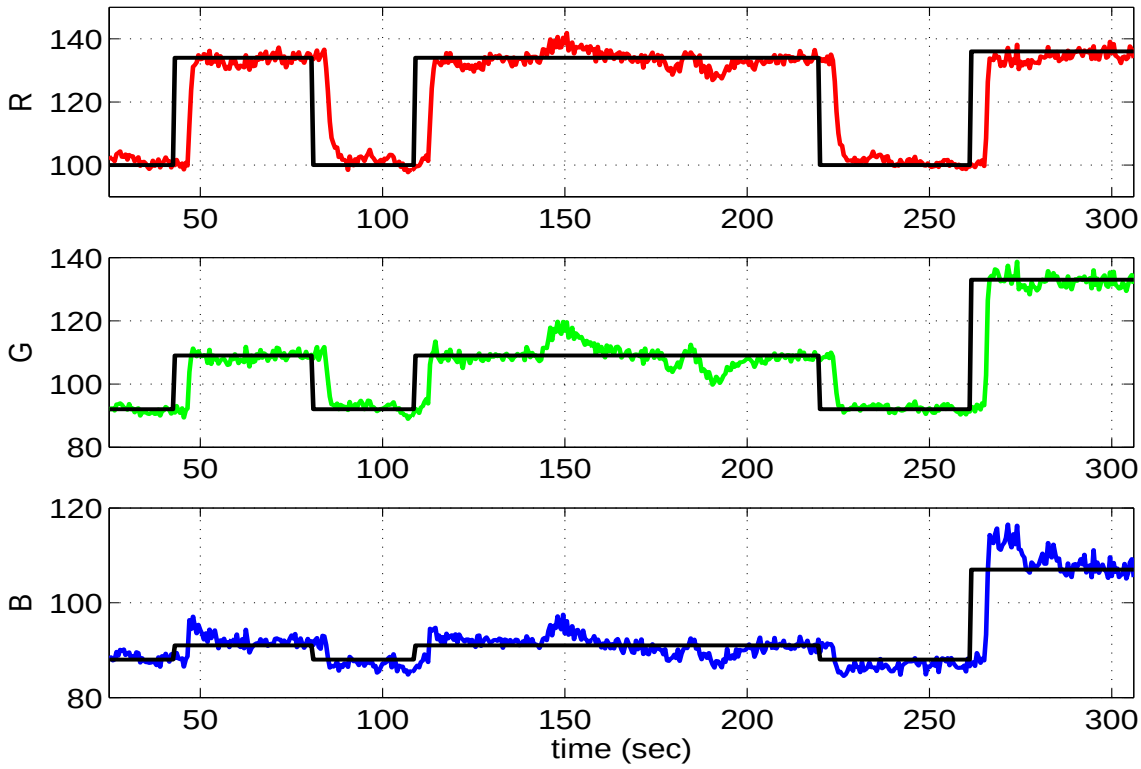

Fig. 3. Experiment 1, optimizing controller: RGB values (measured and reference).

proposed controller can be compared with the use of three well-tuned SISO PI-controllers, cf. Figures 6 - 7. The PI-controller leads to sluggish response because they must be tuned somewhat conservatively due to the static nonlinearities, and they lead to significantly larger transients because they do not account for all couplings in the plant. The pairing of the three SISO controllers was performed using the Relative Gain Array (RGA) method.

VI. Conclusions

A nonlinear optimizing controller for blending processes was developed using a CLF approach, essentially by augmenting a CLF with an objective function for the parameter θ that characterizes the equilibrium point. These results also hold in the case of having an observer that takes into account the effect of the uncertainty and time delay associated to the real plant. Real-time experiments have illustrated the feasibility and good performance of the proposed approach. The results are readily generalizable to over-actuated problems, see [9] for some results and a simulation example of a colorant process when there are more than 3 colorants available. The CLF design idea is borrowed from the area of nonlinear and adaptive control [8] where θ usually denotes unknown parameters to be adapted.

References

[1] A. Diaz and J.A. Barsamian, "Meet changing fuel requirements with online blend optimization," *Hydrocarbon Processing*, , no. 2, pp. 71–76, 1996.

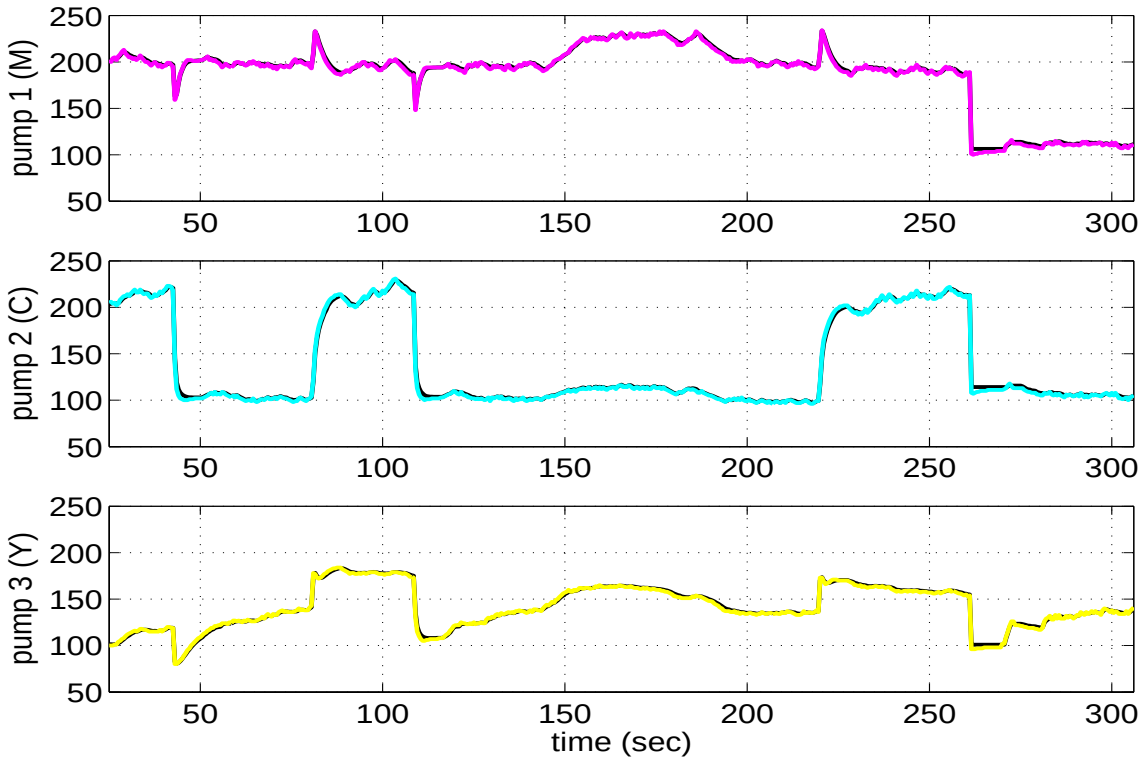

Fig. 4. Experiment 1, optimizing controller: Optimized pump speed values (rpm).

[2] A. Singh, J. F. Forbes, P. Vermeer, and S.S. Woo, "Model-based real-time optimization of automotive gasoline blending operations," *J. Process Control*, vol. 10, pp. 43–58, 2000.

[3] J. Alvarez-Ramirez, A. Morales, and R. Suarez, "Robustness of a class of bias update controllers for blending systems," *Ind. Eng. Chem. Res.*, vol. 41, pp. 4786–4793, 2002.

[4] M. Huzmezan, G.A. Dumont, W. A. Gough, T. Janiewicz, S. Kovac, and D. Meade, "A multivariable Laguerre-based indirect adaptive predictive controller applied to a fuel blending process," in *AdConIP, Kumamoto, Japan*, 2002.

[5] A. Haurani, O. Taha, H. Michalska, and B. Boulet, "Multivariable control of a paper coloring process: A case of study," in *American Control Conference*, Arlington, VA, June, 2001.

[6] S. Chen, T. Murphy, and R. Subbarayan, "A color measurement and control system for paper-making process," in *IEEE Int. Conference on Control applications*, Dearborn, MI, September, 1996.

[7] P. R. Belanger, "Linear-programming approach to color-recipe formulation," *Journal of the Optical Society of America*, vol. 64, no. 11, pp. 1541–1544, 1974.

[8] M. Krstic, I. Kanellakopoulos, and P. Kokotovic, *Nonlinear Adaptive Control Design*, Wiley and Sons, 1995.

[9] T. A. Johansen and D. Sbárbaro, "Optimizing control of over-actuated linear systems with nonlinear output maps via control Lyapunov functions," in *European Control Conference, Cambridge, UK*, 2003.

[10] M. Cannon and B. Kouvaritakis, "Efficient constrained model predictive control with asymptotic optimality," in *Proc. IEEE Conf. Decision and Control, Las Vegas*, 2002, pp. ThA12–1.

[11] P. O. M. Scokaert, D. Q. Mayne, and J. B. Rawlings, "Suboptimal model predictive control (feasibility implies stability)," *IEEE Trans. Automatic Control*, vol. 44, pp. 648–654, 1999.

[12] B.-G. Jeong, K.-Y. Yoo, and Hyun-Ku Rhee, "Nonlinear model predictive control using a Wiener model of a continuous MMA polymerization reactor," *Ind. Eng. Chem. Res.*, vol. 40, pp. 5968–5977, 2001.

[13] H. H. J. Bloemen, C. T. Chou, T. J. J. van den Boom, V. Verdult, M. Verhaegen, and T. C. Backx, "Wiener model identification and predictive control for dual

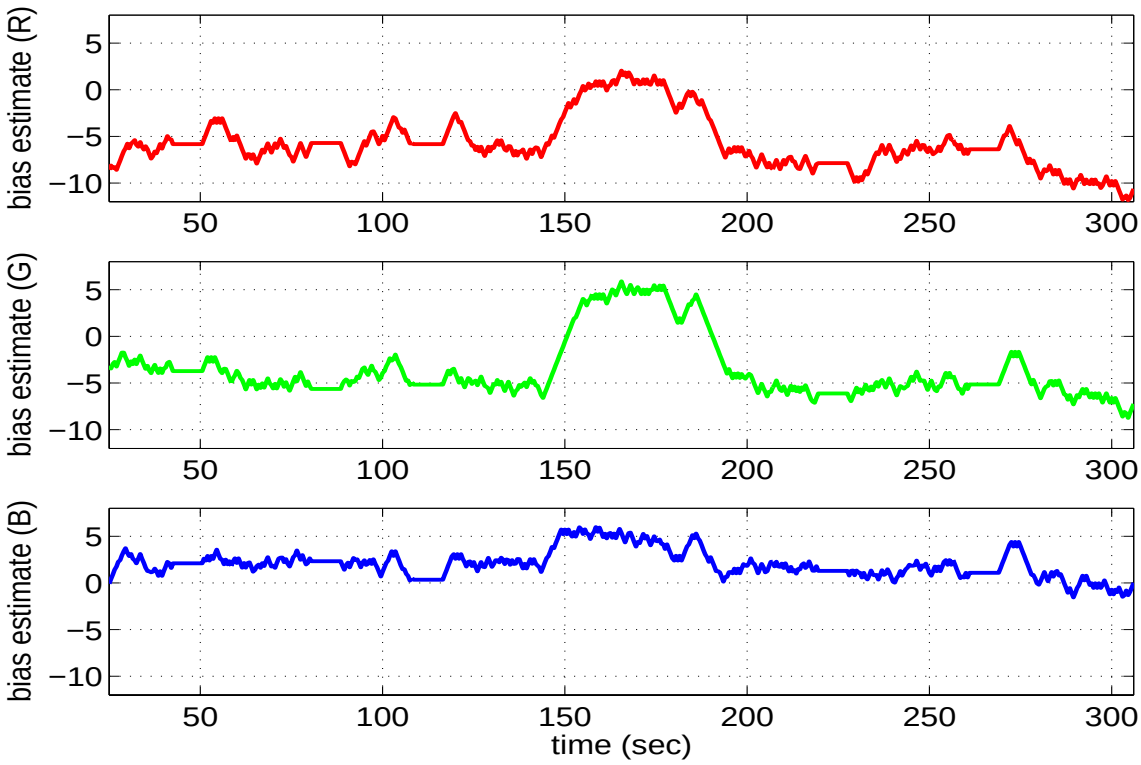

Fig. 5. Experiment 1, optimizing controller: Bias estimates

composition control of a distillation column," *Journal of Process Control*, vol. 11, pp. 601–620, 2001.

[14] S.J. Norquay, A. Palazoglu, and J.A. Romagnoli, "Application of Wiener model predictive control (WMPC) to pH neutralization experiment," *IEEE Trans. Control Systems Technology*, vol. 7, pp. 437–445, 1999.

[15] E. Allen, "Basic equations used in computer color matching," *J. Optical Society America*, vol. 56, pp. 1256–1259, 1960.

[16] J. Nocedal and S. J. Wright, *Numerical Optimization*, Springer-Verlag, New York, 1999.

[17] A. V. Fiacco and G. P. McCormick, *Nonlinear programming: Sequential unconstrained minimization techniques*, J. Wiley and sons, New York, 1968.

[18] H. K. Khalil, *Nonlinear Systems*, Macmillan, New York, 1992.

[19] M. Morari and E. Zafiriou, *Robust process control*, Prentice-Hall, Englewood Cliffs, NJ, 1989.

[20] R. Abrahamson, J. E. Marsden, and T. Ratiu, *Manifolds, Tensor Analysis and Applications (2nd Edition)*, Springer-Verlag, New York, 1988.

[21] C. Kravaris and R. A. Wright, "Deadtime compensation for nonlinear processes," *AIChE Journal*, vol. 35, pp. 1535–1542, 1989.

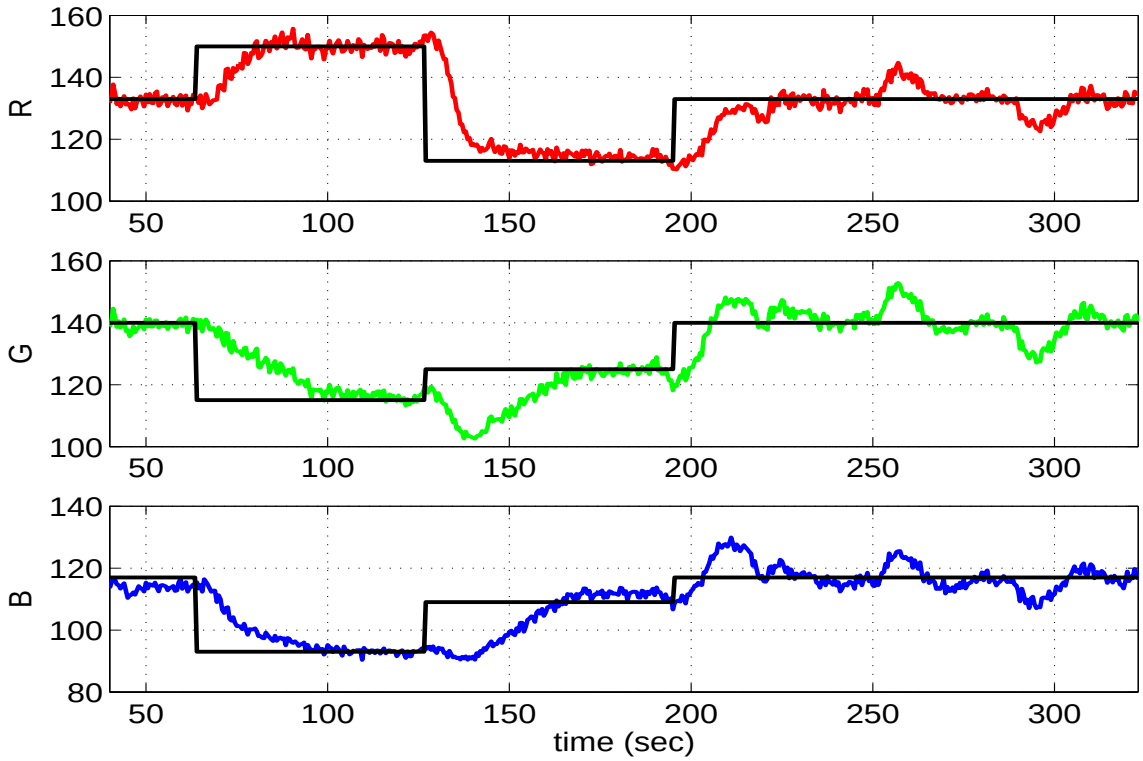

Fig. 6. Experiment 2, PI-controller: RGB values (measured and reference).

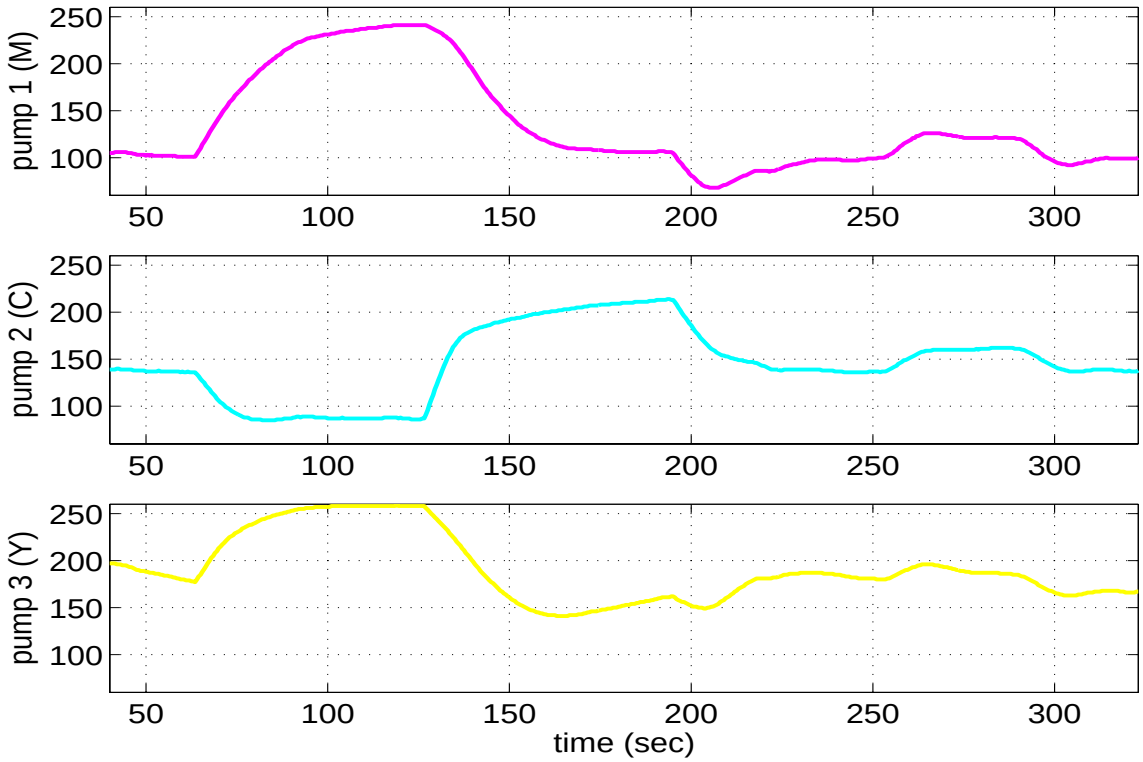

Fig. 7. Experiment 2, PI-controller: Pump speed values (rpm).